

²⁵ Tasi, J., Feldman, A., and Stang, D. A., "The Buckling Strength of Filament-Wound Cylinders Under Axial Compression," CR-266, July 1965, NASA.

²⁶ Holston, A., Jr., Feldman, A., and Stang, D. A., "Stability of Filament Wound Cylinders Under Combined Loading," AFFDL TR 67-55, July 1965, Wright-Patterson Air Force Base.

²⁷ Card, M. F., "Experiments to Determine the Strength of Filament-Wound Cylinders Loaded in Axial Compression," TN D-3522, Aug. 1966, NASA.

²⁸ Singer, J., private correspondence, Nov. 1968 Haifa, Israel.

²⁹ Singer, J., "The Influence of Stiffener Geometry and Spacing on the Buckling of Axially Compressed Cylindrical and Conical Shells," Technion-Israel Institute of Technology, Dept. of Engineering Report TAE-68, Oct. 1967, Air Force Office of Scientific Research.

³⁰ Becker, H., Gerard, G., and Winter, R., "Experiments on Axial Compressive General Instability of Monolithic Ring-Stiffened Cylinders," *AIAA Journal*, Vol. 1, No. 7, July 1963, pp. 1614-1618.

³¹ Lundquist, E. E., "Strength Test of Thin-Walled Duralumin Cylinders in Compression," Rept. 473, 1933, NACA.

³² Ballerstedt, W. and Wagner, H., "Versuche über die Festigkeit dünner unversteifter Zylinder unter Schub- und Längs Kräften," *Luftfahrt-Forschung*, Vol. 13, Sept. 1936, pp. 309-312.

³³ Kanemitsu, S. and Nojima, N. M., "Axial Compression Test of Thin-Walled Circular Cylinders," thesis submitted for the degree of Master of Science in Aeronautical Engineering to the California Inst. of Technology, 1939.

³⁴ Weingarten, V. I., Morgan, E. J., and Seide, P., "Elastic Stability of Thin-Walled Cylindrical and Conical Shells Under Combined Internal Pressure and Axial Compression," *AIAA Journal*, Vol. 3, No. 6, June 1965, pp. 1118-1125.

³⁵ Dow, M. B. and Peterson, J. P., "Bending and Compression Tests of Pressurized Ring-Stiffened Cylinders," TN D-360, April 1960, NASA.

³⁶ Fung, Y. C., and Sechler, E. E., "Buckling of Thin-Walled Circular Cylinders Under Axial Compression and Internal Pressure," *Journal of the Aeronautical Sciences*, Vol. 24, May 1957, pp. 351-356.

³⁷ Lo, H., Crate, H., and Schwartz, E. B., "Buckling of Thin Walled Cylinder Under Axial Compression and Internal Pressure," Rept. 1027, 1951, NACA.

JUNE 1970

J. SPACECRAFT

VOL. 7, NO. 6

Adjustment of a Thermal Mathematical Model to Test Data

JOCHEN DOENECKE*

European Space Research and Technology Centre, Noordwijk, Holland

An iteration method is presented by which a thermal mathematical model of a spacecraft can be adjusted to measured temperatures by minimizing the sum of the squares of the residuals of the nodal heat balance equations. The method permits a common treatment of three cases, in which the number of unknowns in the system of equations is smaller than, equal to, or larger than the number of equations. These cases may occur in any of four conditions of test; 1) steady-state, 2) cooling from steady-state, 3) cyclic state (repeated, periodic, cooling and heating), and 4) arbitrary transient heating. The 93-node model of the ESRO-I satellite is analyzed. The foregoing four test conditions and a total number of 16,089 temperatures at two attitudes of the spacecraft (horizontal and vertical position) with respect to solar radiation are used to recalculate 7 sets of 1957 unknown factors with a digital computer. The adjustment reduces the sum of the residuals of the heat balance equations in the steady-state tests by a factor of 5, and in all transient tests by a factor of 2. The rms of the differences between the measured and calculated temperatures and the standard deviation of these differences are also reduced by a factor of 2 when a model found from a cyclic state is applied to other tests. It is observed that the best verification of any spacecraft model is possible from such a state.

Nomenclature

| | |
|----------|---|
| a | = known coefficient in general system of equations |
| A | = radiation factor to space, $w/({}^{\circ}\text{K})^4$ |
| A' | = area, m^2 |
| b | = known factor in general system of equations |
| B | = heat capacity, $w\text{-sec}/{}^{\circ}\text{K}$ |
| B' | = absorption or "Gebhart" factor |
| c | = specific heat, $w\text{-sec}/\text{kg}\cdot{}^{\circ}\text{K}$ |
| C | = thermal conductance, $w/{}^{\circ}\text{K}$ |
| D | = temperature-time derivative, ${}^{\circ}\text{K}/\text{sec}$ |
| E | = "Earth" radiation, w |
| FE, FS | = weighting factors defining how the corrections are distributed among the unknowns E, S , respectively |
| G | = matrix used in Eqs. (4) and (5) |

| | |
|----------|--|
| IAV | = integer array specifying how the equations are to be averaged |
| KOI | = integer specifying the type of test |
| KTE | = number of equations for which $S = 0$ in the cyclic state |
| M | = number of instants or moments |
| N | = number of nodes |
| NAV | = number of averaged equations |
| NC | = number of independent conductances |
| NE | = number of equations in the general system |
| NPO | = number of points on a temperature-time curve |
| NU | = number of unknowns in the general system |
| NR | = number of independent radiation factors |
| NS | = number of skin nodes |
| r | = residual in heat balance equation, w |
| R | = radiation factor, $w/({}^{\circ}\text{K})^4$ |
| RE, RS | = ranges specifying the hypervolume in which the unknowns E, S , respectively, are allowed to vary |
| s | = sum of all terms in the heat balance equation, w |
| S, S' | = solar radiation, w , and solar flux, w/m^2 , respectively |
| t | = time, sec |

Received July 16, 1969; revision received January 26, 1970. The author would like to thank A. Accensi for illuminating discussions and helpful comments.

* Structures Division.

| | |
|--------------------|--|
| T | = temperature, °K |
| V | = volume |
| x | = unknowns in general system of equations |
| α, ϵ | = absorptivity and emissivity, respectively |
| μ, ν | = standard deviation, and rms, respectively, of differences between measured and calculated temperatures |
| ρ | = density |
| σ | = Stefan-Boltzmann constant |

Subscripts

| | |
|--------|-----------------------------------|
| i, j | = of or on node i ; of node j |
| m | = at instant or moment m |
| ji | = from node j to node i |
| is | = from node i to space |
| w | = wall |

Superscripts

| | |
|----------|---|
| ca, me | = calculated and measured, respectively |
| n, o | = new and original values, respectively |

Introduction

SINCE the thermal control of the nonspinning ESRO-I spacecraft was critical, it had been divided into a relatively large number of nodes (93) and the thermal mathematical model had been calculated with great care.¹ During the two-week thermal-balance test, the various test requirements (constant temperatures, reproducibility of the period, constant intensity distribution of simulated solar radiation, etc.) were fulfilled in every respect.² Nevertheless, the rms of the differences between the calculated and the measured temperatures was of the order of 10°C. This paper describes an attempt to adjust all 1957 factors of the model, (except for a few internal exchange factors representing negligible contributions to the heat balances) by an automatic method employing a computer.

First the parameters are changed according to specified weighting factors, estimated from a physical judgement of the problem, so that the total heat balance over the spacecraft and the test period is fulfilled. Then the normal equations of the heat balances of the nodes are written,³ and the Gauss-Seidel iteration technique⁴ is applied to this system. Reasonable physical limits or ranges of the parameters are established, and the solution is sought only within these limits. This is only one of the numerous techniques by which a model can be adjusted to test data. The other methods try to minimize the differences of calculated and measured temperatures and (or) investigate special phenomena such as correlations, experimental errors and sensitivities. As a result of this study the adjustments for seven different test conditions, and the extent to which a set of factors obtained from one test condition represents other conditions, are discussed.

Formulation of Problem and Solution by Iteration

If in a test chamber the simulated solar radiation is constant, no power is dissipated in the spacecraft, and no albedo and planetary radiations are simulated, one can write the heat balance of the node i at the moment m in the form,

$$E_i + S_i - A_i T_{i,m}^4 - B_i D_{i,m} + \sum_{j=1}^N C_{ji} (T_{j,m} - T_{i,m}) + \sum_{j=1}^N R_{ji} (T_{j,m}^4 - T_{i,m}^4) = 0 \quad (1)$$

where

$$E_i = \sigma \epsilon_i A'_i B'_{is} T_w^4 = \text{energy absorbed by node } i \text{ owing to a nonzero temperature of the chamber walls, } w$$

$$S_i = S' A'_i \alpha_i = \text{energy absorbed by node } i \text{ owing to the simulated solar radiation, } w$$

$$A_i = \sigma \epsilon_i A'_i B'_{is} = \text{radiation factor to space, } w/(\text{°K})$$

$$B_i = (\rho V)_i = \text{heat capacity, } w\text{-sec/°K}$$

$$D_{i,m} = (dT/dt)_{i,m} = \text{temperature-time derivative, °K/sec}$$

$$R_{ji} = \sigma \epsilon_j A'_j B'_{ji} = \text{radiative heat exchange factor between node } i \text{ and node } j, w/(\text{°K})^4$$

Equations (1) have to be satisfied for all nodes ($i = 1, \dots, N$) and all times ($m = 1, \dots, M$). The cooling of the shroud is assumed to be so strong that its emission [term E_i in Eqs. (1)] can be supposed constant and independent of the solar simulator. The manner in which the matrices $T_{i,m}$, $T_{i,m}^4$ and $D_{i,m}$ are built up from the measurements is explained later. When they are introduced into Eqs. (1), the latter are usually not satisfied. The sum of the squares of the right-hand sides or residuals $r_{i,m}$,

$$\phi = \sum_{m=1}^M \sum_{i=1}^N r_{i,m}^2 \quad (2a)$$

is then used as an optimization criterion. We call the adjusted model that which minimizes ϕ .

Before explaining how the minimum of ϕ is sought when the equations are given in the form (1), we shall treat the procedure for a general linear system. Equations (1) can be written in the form:

$$\sum_{j=1}^{NU} a_{ij} x_j - b_i = 0 \text{ (or } = r_i), \quad i = 1, \dots, NE \quad (3)$$

where NU is the number of unknowns x . In a steady-state test the number of equations NE equals N . In a transient test we may write $NE = N \cdot M$, but we have to realize that when the time interval between the measurements (Δt) has not been sufficiently high, the equations may be linearly dependent or ill-conditioned. The factors a represent the known coefficients (given by the matrices $T_{i,m}$, $T_{i,m}^4$ or $D_{i,m}$). The factors b represent the sum of the known terms in each equation, and will only appear for a case in which the values of some factors of the model are considered to be established. Three cases may occur in the system (3), a) when $NE < NU$, many solutions may be possible, b) when $NE > NU$, there is usually no one solution that exactly satisfies the system Eqs. (1) or (3), and one can only minimize ϕ [Eq. (2a)], and c) when $NE = NU$, an exact solution may exist. When passing from a steady-state to a transient test, NU increases much less than NE, because then only the unknown heat capacities B_i in Eqs. (1) have to be included. The method to be found should permit a common treatment of all cases. Solutions which are not physically meaningful should be excluded. The "minimum" of ϕ is found by applying the Gauss-Seidel iteration technique to the normal equations. We have not given a proof that this method always converges to the absolute minimum of ϕ ; nevertheless, it always converges when the diagonal elements in a system of equations are large compared with the off-diagonal elements in its row or equation.⁴ In our case, an internal conductance or radiation factor occurs (in a steady-state test) only in two equations (corresponding to two nodes), while all the other factors occur only in one equation (corresponding to one node) and can thus be considered to belong to the diagonal terms in the system. We have done computations for several small models. The convergence has always been very rapid.

The r_i from Eqs. (3) are introduced into

$$\phi = \sum_{i=1}^{NE} r_i^2 \quad (2b)$$

Putting $\partial\phi/\partial x_1 = 0$, $\partial\phi/\partial x_2 = 0$, ..., $\partial\phi/\partial x_{NU} = 0$ gives the system

$$x_i \sum_{k=1}^{NE} a_{k,i}^2 + \sum_{j=1}^{NU} \left(x_j \sum_{k=1}^{NE} a_{k,i} a_{k,j} \right) - \sum_{k=1}^{NE} a_{k,i} b_k = 0, \quad i = 1, \dots, NU$$

which is solved by iteration,

$$x_i = G_{i,i} - \sum_{j=1, j \neq i}^{NU} x_j G_{i,j}, \quad i = 1, \dots, NU \quad (4)$$

where

$$G_{i,i} = \sum_{k=1}^{NE} a_{k,i} b_k / d_i, \quad d_i = \sum_{k=1}^{NE} a_{k,i}^2 \quad (5a)$$

$$G_{i,j} = \sum_{k=1}^{NE} a_{k,i} a_{k,j} / d_i, \quad \text{for } i \neq j \quad (5b)$$

The matrix $G_{i,j}$ in Eq. (4) can be stored in the memory of the digital computer. The optimum solution is sought within the NU-dimensional experimental region (from now on called the hypervolume) defined by the specified ranges of the unknowns. Therefore, after each application of Eq. (4) a check is made to see whether the x_i value just calculated is within the specified hypervolume; if not, it is put equal to the specified boundary which it exceeds.

When the operations performed are the same as those just described, but Eqs. (1) and (2a) are used instead of Eqs. (3) and (2b), respectively, a conductance, say $C_{2,4}$ between nodes 2 and 4, is calculated by

$$C_{2,4} = (Ex_1 + Ex_2) / 2 \sum_m (T_{4,m} - T_{2,m})^2 \quad (6)$$

where

$$Ex_1 = \sum_{m=1}^M \left[\left\{ -E_2 - S_2 + A_2 T_{2,m}^4 + B_2 D_{2,m} - \sum_{j=1, j \neq 4}^N C_{j,2} (T_{j,m} - T_{2,m}) - \sum_{j=1}^N R_{j,2} (T_{j,m}^4 - T_{2,m}^4) \right\} (T_{4,m} - T_{2,m}) \right]$$

Ex_2 is obtained by interchanging suffixes 2 and 4 in the expression Ex_1 . The unknown factor A_i of Eq. (1) is calculated from

$$A_i = \sum_{m=1}^M [(E_i + S_i - B_i D_{i,m} + q) T_{i,m}^4] / \sum_m (T_{i,m}^4)^2 \quad (7)$$

where

$$q = \sum_{j=1}^N \{ C_{j,i} (T_{j,m} - T_{i,m}) + R_{j,i} (T_{j,m}^4 - T_{i,m}^4) \}$$

An equation similar to Eq. (6) can be written for an unknown radiation factor R_{ij} , and equations similar to Eq. (7) can be written for the unknown factors E_i , S_i , and B_i . In Eq. (6) the reciprocity law ($C_{ij} = C_{ji}$) is considered.

Equations such as Eqs. (6) and (7) are modified in order to reduce the computer time. Their numerators are not calculated as a function of the coefficients of system (1), but as a function of the old (superscript o) residuals. The equations finally programmed read,

$$C_{ij}^n = \frac{- \sum_m \{ [r_{i,m}^o - C_{ij}^o (T_{j,m} - T_{i,m})] (T_{j,m} - T_{i,m}) + [r_{j,m}^o - C_{ij}^o (T_{i,m} - T_{j,m})] (T_{i,m} - T_{j,m}) \}}{2 \sum_m (T_{j,m} - T_{i,m})^2} \quad (8a)$$

$$r_{i,m}^n = r_{i,m}^o + (C_{ij}^n - C_{ij}^o) (T_{j,m} - T_{i,m}),$$

$$r_{j,m}^n = r_{j,m}^o - (C_{ij}^n - C_{ij}^o) (T_{j,m} - T_{i,m}), \quad (9a)$$

$$i = 1, \dots, N, j = 1, \dots, N$$

$$B_i^n = \sum_m [(r_{i,m}^o + B_i^o D_{i,m}) D_{i,m}] / \sum_m D_{i,m}^2 \quad (8b)$$

$$r_{i,m}^n = r_{i,m}^o - (B_i^n - B_i^o) D_{i,m}, \quad i = 1, \dots, N \quad (9b)$$

$$S_i^n = - \sum_m (r_{i,m}^o - S_i^o) / (NAV - KTE) \quad (8c)$$

$$r_{i,m}^n = r_{i,m}^o + S_i^n - S_i^o, \quad i = 1, \dots, NS \quad (9c)$$

The equations for R_{ij} , A_i , and E_i are not presented. They are similar to Eqs. (8a-8c) respectively. At first C_{ij} and R_{ij} are corrected in a double loop and then B_i , S_i , E_i , and A_i are corrected in a single loop. The reason for selecting this sequence of computation is explained later. The difference between the old and new values (superscript n) of the factors, given by Eqs. (8), is used to correct the residuals after each step [Eqs. (9)]. The term $NAV - KTE$ in Eq. (8c) is explained later; it covers the fact that the solar radiation input is only adjusted over the time during which the solar simulator is on. Chosen ranges RE, RS, RA, RB, RC, and RR define, together with the initial model, the hypervolume in which the factors E_i , S_i , A_i , B_i , C_{ij} , and R_{ij} are, respectively, allowed to vary.

Preparation of Problem

The following four test conditions are treated: 1) the steady-state, characterized by stationary temperatures (Fig. 1a), and requiring constant test conditions over a long period of time, 2) cooling from steady-state, which occurs when the simulated solar radiation is turned off (Fig. 1a), 3) the "cyclic" state, in which each node has the same temperature at the end of a cooling-plus-heating cycle as it had at the beginning (Fig. 1b). For the fourth term of Eqs. (1) we can then write,

$$\sum_{m=1}^M B_i D_{i,m} = 0, \quad (i = 1, \dots, N) \quad (10)$$

4) arbitrary transient heating, treated because a thermal balance test usually begins with a period which does not correspond to any of the three foregoing cases (Fig. 1c).

Setting Up the System of Equations

To reduce experimental errors and to permit solution of large problems on small computers, we average Eqs. (1) over defined time intervals, such as shown beneath the curves in Figs. 1a and 1b ($m = 1, \dots, NAV$). We do this by specifying NPO, the number of points on the temperature-time curves, NAV, the number of sets (one set covers all nodes) of averaged equations desired, IAV, an integer array defining the lengths of the time intervals and KTE, an integer needed to specify the length of the cooling period in the cyclic state. The derivatives $D_{i,m}$ at the points 1, 2, ..., NPO are simply calculated by the midpoint slope method. For that purpose the temperatures at the intermediate points a, b, \dots, f (Fig. 1b) are calculated as the arithmetic means of the adjacent points and the time interval Δt between the measurements is chosen constant. Because in the matrices that need

to be built up ($T_{i,m}$, $T_{i,m}^4$ and $D_{i,m}$) the column number m varies owing to the averaging process from 1 to NAV, but not from 1 to NPO ($NAV < NPO$), it is an advantage not to store all temperatures simultaneously in the memory of the computer. When a set of temperatures (for one instant) is read, some calculations are made and values stored in the

matrices before the next set is read. In the case illustrated by Fig. 1a the whole computation process is first done for the steady-state (using point 1 only) and the matrices are then built up (using points 2-10).

The specification of the integer array IAV can be avoided by calculating the sums of all terms in Eqs. (1),

$$s_{i,m} = E_i + S_i + A_i T_{i,m}^4 + B_i |D_{i,m}| + \sum_j C_{ji} |T_{j,m} - T_{i,m}| + \sum_j R_{ji} |T_{j,m}^4 - T_{i,m}^4| \quad (11)$$

Then IAV is automatically calculated so that $\sum_m \sum_i s_{i,m}$ have nearly the same value when summed over each time interval. This procedure ensures that the same weighting is associated with all equations. For this reason, when this automatic procedure is not used, one should in the cyclic state, construct as many equations from the cooling period as from the heating period (Fig. 1b).

Adjustment of the Model to Satisfy the Over-All Heat Balance

If Eqs. (1) are summed over all nodes, the 5th and 6th terms are eliminated at each instant m . We can use this fact for a simultaneous correction of the remaining four types of factors only by summing, also over all instants,

$$\sum_m \sum_i (E_i + S_i - A_i T_{i,m}^4 - B_i D_{i,m}) = 0 \quad (12)$$

Let us call E, S, A , and B the sums (over all nodes and instants) of the four terms in Eq. (12), and FBE, FBS, FBA, and FB the chosen weighting factors, which define how the corrections are, respectively, distributed to these sums. These weighting factors can be specified so that their sum is unity and should be chosen according to a physical judgment of the problem. The left-hand side of Eq. (12) is the total residual, r , which should be reduced to zero. The following equations are used to calculate the corrections $\Delta E, \Delta S, \Delta A$, and ΔB of the preceding four sums, respectively,

$$\frac{\Delta B}{|B|} = \frac{\Delta E}{E} \frac{FB}{FBE} = \frac{\Delta S}{S} \frac{FB}{FBS} = \frac{\Delta A}{A} \frac{FB}{FBA} \quad (13)$$

$$\Delta B + \Delta E + \Delta S + \Delta A = r \quad (14)$$

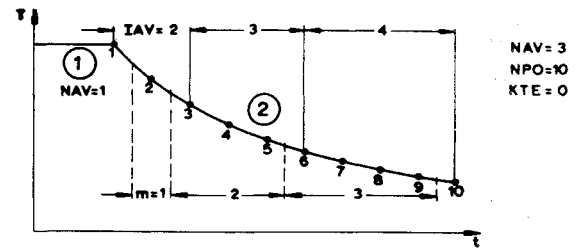
The absolute value of B is used since the derivative $D_{i,m}$ can either be positive or negative. After calculating E, S, A , and B , one can determine one of the corrections, e.g., ΔB , by Eqs. (13) and (14). The other three corrections $\Delta E, \Delta A$, and ΔS can then be found by Eqs. (13). The corrections are distributed to the different nodes in proportion to the initial values,

$$S_i^n = S_i^o - S_i^o(\Delta S/S), \quad E_i^n = E_i^o - E_i^o(\Delta E/E) \quad (15a)$$

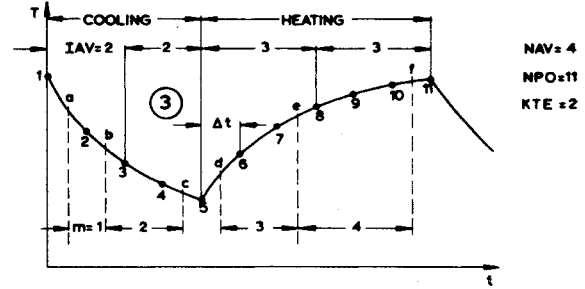
$$A_i^n = A_i^o + A_i^o(\Delta A/A), \quad B_i^n = B_i^o + B_i^o(\Delta B/B) \quad (15b)$$

The 4th term in Eq. (12) is zero in the steady-state and cyclic tests provided that in the cyclic state the intervals over which the summation is made are constant. Because this is not generally the case, we correct in the steady-state only E, S , and A by defining the corresponding weighting factors FE, FA, and FS (B left out), and in all transient tests we also correct the capacities.

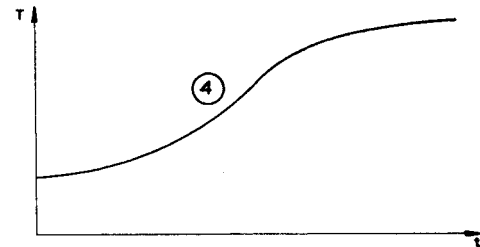
Equations (13-15) are applied before the actual adjustment procedure described by Eqs. (8) and (9) begins and also after each run through these equations. Because the E_i, S_i, A_i , and B_i are already corrected by Eqs. (13-15), we start in Eqs. (8) and (9) with the correction of the nodal exchange terms followed by the most uncertain supposed factors of each node.



a) Steady state, and cooling from steady state



b) Cyclic state



c) Arbitrary transient heating

Fig. 1 Temperature (T) of a node as a function of time (t) for four different conditions of test.

Adjustment of a 93-Node Model

Review of Test and Assumptions Made for the Analysis

The nearly cylindrical ESRO-I spacecraft (diameter, 76 cm; height, 93 cm) was suspended in a space chamber by wires first in a vertical and then in a horizontal position.² In the vertical (horizontal) position the simulated solar radiation was normal (parallel) to the main axis of symmetry. From the total test duration of two weeks, the seven test periods in Table 1, representing characteristic conditions, were selected and analyzed.

The temperatures at the end of each cycle in tests V-3 and H-3 were, with a maximum deviation of 0.5°C , those at the beginning (for all nodes). A cooling period of 36 min, followed by a heating period of 64 min, was repeated 12 times in order to obtain this condition. Temperatures were only measured for 80 of the 93 nodes; the others were estimated from those of immediately adjacent nodes or those at symmetrically equivalent locations. Before these temperatures were used, the model was carefully reviewed. The model described in Ref. 1 gave for ν (the rms of the differences between the calculated and measured temperatures) in the steady-state tests (V-1 and H-1) 10.8° and 16.1°C , respectively.² This model was adjusted by simply looking at the deviations and trying different combinations of the parameters. After about 30 computer runs, the ν 's were reduced to 8.7 and 11.0°C , respectively.²

This adjusted model was used (considering differences and later changes on the flight model) for the orbit predictions and development of the project and was certainly adequate

Table 1 The seven cases analyzed

| Test ^a | NPO | Δt , min |
|-------------------|---------|------------------|
| V-1 | 1 | ÷ |
| V-2 | 22 (+1) | 2 |
| V-3 | 51 | 2 |
| V-4 | 25 | 5 |
| H-1 | 1 | ÷ |
| H-2 | 22 (+1) | 2 |
| H-3 | 51 | 2 |
| $\Sigma = 173$ | | |

^a V = vertical; H = horizontal; 1-4 are the four test conditions (see text and Fig. 1).

for that purpose. To find out whether the ν 's could be further reduced, it was preferred to start from the original model of Ref. 1 rather than from the adjusted one of Ref. 2. The original model was checked again and the following modifications were made, 1) one radiation factor was replaced by a 48% smaller value, 2) some small radiation factors and conductances were left out, 3) all conductances were reconsidered and recalculated if necessary (it is felt that the new values are closer to the physical reality), and 4) the

Table 2 Periods over which the equations are averaged

| Test | NAV | IAV | KTE |
|----------|-----|-------------------------|-----|
| V-1, H-1 | 1 | | 0 |
| V-2, H-2 | 5 | 2, 3, 4, 6, 7 | 0 |
| V-3, H-3 | 8 | 3, 4, 5, 6, 6, 7, 9, 10 | 4 |
| V-4 | 5 | 2, 3, 5, 6, 8 | 0 |

"effective" emissivity (value by which a view factor between two surfaces has to be multiplied to give the net heat exchange) of 0.7 was chosen for the internal links of all the nodes as in Ref. 2 and not 0.9 as in Ref. 1, because the over-all heat exchange was found to be overestimated. The number of parameters finally left in the model was: $NU = 3.40$ (NS) + 93 (N) + 175 (NC) + 1569 (NR) = 1957, where NC and NR are, respectively, the number of nonzero C_{ij}

Table 3 Sums of all unknown factors of 9 models^a

| Model | $\Sigma S_{i,0}$ | ΣS_i | ΣE_i | $\Sigma A_i \cdot 10^8$ | $\Sigma B_i \cdot 10^{-2}$ | ΣC_i | $\Sigma R_i \cdot 10^8$ |
|-------|------------------|--------------|--------------|-------------------------|----------------------------|--------------|-------------------------|
| 0 | | | 5.25 | 9.17 | 558 | 14.1 | 13.3 |
| V-1 | 415 | 451 | 5.41 | 9.08 | | 12.7 | 13.3 |
| V-2 | | | 4.90 | 9.86 | 433 | 12.3 | 12.8 |
| V-3 | 415 | 447 | 5.29 | 9.09 | 467 | 12.9 | 13.2 |
| V-4 | 415 | 462 | 5.43 | 8.96 | 547 | 12.0 | 12.9 |
| V-4s | 415 | 470 | 5.42 | 8.96 | 527 | 12.1 | 12.9 |
| H-1 | 384 | 410 | 5.23 | 9.21 | | 12.3 | 12.8 |
| H-2 | | | 4.76 | 10.10 | 407 | 11.9 | 12.9 |
| H-3 | 396 | 392 | 5.24 | 9.18 | 421 | 10.6 | 12.0 |

^a In all tables the units are those given in the Nomenclature.

and R_{ij} above the diagonal in the matrices. This model gave for the two steady-state tests $\nu = 10.6^\circ$ and 9.84°C , respectively. It was felt that a significantly better agreement based on further physical judgements and checkings alone is not possible. This model was always used as the initial one in this study.

Owing to the large number of computations involved, it was decided to make the adjustments to the seven tests of

Table 4 Correction factors (from model V-3) for ΣS_i and ΣA_i

| | Nodes | M_0 | M_{V-3}/M_0 |
|--------------|-------|-------|---------------|
| ΣS_i | 13-14 | 5.44 | 1.114 |
| | 1-6 | 109.2 | 1.055 |
| | 17-22 | 100.1 | 1.078 |
| ΣA_i | 13-16 | 0.04 | 0.974 |
| | 1-12 | 2.82 | 0.992 |
| | 17-28 | 2.82 | 0.996 |

Table 1 for one set of the ranges, weighting factors and averaging periods (IAV) only, and first roughly to investigate their influence. Let us first comment on the preliminary studies and the choice of the set. When using Eq. (12) we found that the total heat balances over the spacecraft for the two steady-state tests were low by 45.3 and 33.4 w, respectively. Because changing only one of these three types of parameters, S_i , E_i , or A_i , would imply corrections larger than could be explained by simple inaccuracies or measuring errors, all three were assumed to need correction. The weighting factors were chosen according to the estimated relative errors (and importance) of the types of parameters and the ranges were chosen according to the estimated absolute errors. The ranges had to be so large that the model obtained after the first use of Eqs. (13-15) was still, in all test conditions, within the specified limits. Because it was stated that by the use of Eqs. (13-15) the term $|\Sigma_m \Sigma_{i,m}|$ was only slightly reduced and because $r_{i,m}$ of the 53 inner nodes is independent of the corrections made by these equations, it was concluded that the largest inaccuracies were probably in the R_{ij} and C_{ij} factors. Therefore their ranges were chosen largest. The calculations (not presented here) showed that the choice of the limits or ranges was more important than that of the weighting factors. Larger limits permit greater reduction of the residuals, but are more likely to give parameters further from the physical reality than the initial model and increase the risk that a model found from one test is not so representative for other tests. The choice of IAV had the least importance.

The weighting factors were chosen to be $FE = 0.32$, $FS = 0.53$, $FA = 0.15$, $FBE = 0.26$, $FBS = 0.27$, $FBA = 0.122$ and $FB = 0.348$. The chosen ranges were $RE = 1.09$, $RS = 1.12$, $RA = 1.06$, $RB = 1.35$, $RC = 1.7$, and $RR = 1.35$. This means, for instance,

$$S_i^o/1.12 \leq S_i^n \leq S_i^o \cdot 1.12$$

The periods over which Eqs. (1) were averaged are given in Table 2.

In all 7 tests the calculations were started with the initial model except for tests V-2 and H-2, in which the adjustment process began with the models found from tests V-1 and H-1, respectively. The number of iterations was 5 for all tests.

Results of the Analysis

The initial model is characterized by a zero, the model found from test V-1 is called model V-1, etc., and model V-4s (s = short) is based on only the first 35 min (instead of 120 min) of test V-4: IAV = 2, 2, 3. Table 3 presents the sums of all factors of Eqs. (1) for these 9 models. Column 2 contains the sum of all solar fluxes with which the calculations were started in the various tests, and column 3 presents these sums obtained after the adjustment process. Table 3 shows model V-4s is very close to model V-4; consequently, no further calculations with that model were made.

We see from Table 3 that the sum of the heat capacities ΣB_i found from a cooling period (test V-2 or H-2) is lower than that from the cyclic state (test V-3 or H-3, respectively), whereas the sum found from a heating period (test V-4) is higher (than for V-3). This can be explained in the following way. The temperatures are usually measured only on the surface of any mass. In Fig. 2 temperature-time curves for heating and cooling are shown for a point on the surface (subscript 1) and for the average over the whole mass of the node (subscript 2). In both the heating and cooling periods, the difference $|T_1 - T_2|$ at the end of the test time is smaller than the average difference over the time (provided the test time was not very short). Only during the first part of a heating period is $(D_{i,m})_1$ greater than $(D_{i,m})_2$ while $(T_{i,m})_1$ is always greater than $(T_{i,m})_2$. Therefore one can write,

$$\frac{(\sum_m D_{i,m})_1 - (\sum_m D_{i,m})_2}{|(\sum_m D_{i,m})_2|} < \frac{(\sum_m T_{i,m})_1 - (\sum_m T_{i,m})_2}{(\sum_m T_{i,m})_2}$$

In a cooling period, the "less than" in this inequality should be replaced by "greater than." Thus all coefficients in Eqs. (1), when the average over the whole test time is considered, increase (decrease) in a heating (cooling) period relatively more, owing to the measuring error, than the $D_{i,m}$. The effect is the same as if the $D_{i,m}$ are considered to have decreased (increased) and the other coefficients to have remained unaltered. The adjustment method tries to compensate this (and other phenomena) and therefore automatically gives higher (lower) values for the capacities.

Table 3 shows further that for the vertical position the assumed simulated solar radiation was too low, whereas ΣB_i and ΣC_i of the initial model were certainly too high, and ΣR_i was perhaps slightly too high. The over-estimation of the heat capacities can be explained by the way they were determined. They were calculated using tables containing the weight-breakdown for the flight unit. In the tested spacecraft the electronic components were replaced by dummies and some parts were left out, and this was probably not completely allowed for. The reduction of the effective emissivity of the inside to 0.7 was justified, because the radiation factors were still overestimated.

Table 4 shows some characteristic correction factors for ΣA_i (and ΣS_i) for: nodes 13-16 (or 13-14) representing the equator ring, nodes 1-12 (or 1-6) representing the solar panels on the upper half of the spacecraft, and nodes 17-28 (or 17-22) representing the solar panels on the lower half of the spacecraft. (The S_i factors are only summed over the nodes illuminated in the horizontal position.) Column 3 of Table 4 presents the sums of the factors for the initial model, and column 4 gives the ratio, Model V-3/Model 0. Model V-3 was chosen, because the cyclic state permits the most representative determination of the parameters (see also Table 7). The ratios (correction factors) for absorbed solar radiation and emissivity are much farther from unity for the equator ring than for the panels. However, the equator ring had been divided into fewer nodes, and its surface properties were known less accurately than those of the panels.

Table 5 presents the sum of the residuals $\sum_m \Sigma_i r_{i,m}$ and the sum of the absolute residuals $\sum_m \Sigma_i |r_{i,m}|$ as calculated for the models with which the calculations were started and as calculated for the models obtained from the 7 tests. The absolute sum of all terms $\sum_m \Sigma_i s_{i,m}$, as obtained by Eq. (11), is also given for the initial models, because a comparison of this value with $\sum_m \Sigma_i |r_{i,m}|$ gives an idea of how well the initial model fulfills the equations. For all seven tests, $\sum \Sigma |r_{i,m}|$ is considerably reduced by the adjustment process. The reduction is largest for the stationary tests (V-1 and H-1). To compare the various tests, the figures of Table 5 should be divided by NAV of Table 2. Table 6 illustrates, for test V-3, the factors of node 1, the coupling factors between node 1 and 2, and $|\sum \Sigma r_{i,m}|$.

After having found the adjusted models, the temperatures were recalculated for the various tests. Because considerable computer time was required, the temperatures in the

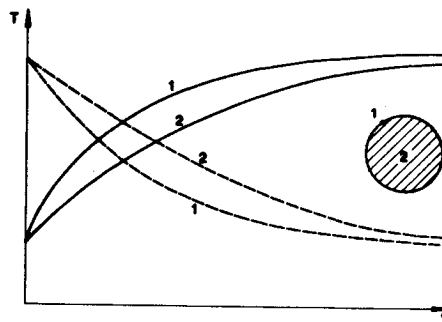


Fig. 2 Temperature-time curves; 1-measured, 2-averaged over the whole mass.

transient tests were calculated only for the first 12 min (25 min in test V-4). In the cyclic state (tests V-3 and H-3) the temperature calculations were made for the first 12 min of the cooling and of the heating period. All transient temperatures were calculated by starting with the measured ones, except in tests V-2 and H-2, where the temperatures calculated in tests V-1 and H-1, respectively, were used. A further modification to this exception was made, because Table 3 shows a relatively large difference between models V-1 and V-2 (and between H-1 and H-2), and because we wanted to see how well the models fitted for the various tests; the measured temperatures were also used as initial ones when model V-2 was applied to test V-2 (and model H-2 to test H-2). When a model, found from a test during which the satellite's position was vertical (horizontal), was applied to a test in which the position was horizontal (vertical), the S_i values of model 0 were used. Otherwise the adjusted S_i values were taken.

Table 3 shows that general shifts between the levels of calculated and measured temperatures might be expected in some cases. Because such shifts can be explained (partly by the measuring errors explained in Fig. 2), a criterion was first calculated by which they were eliminated. This is the standard deviation of the differences between the measured (superscript *me*) and calculated (*ca*) temperatures given by:

$$\mu = \left\{ \frac{1}{N \cdot M} \sum_{m=1}^M \sum_{i=1}^N (T_{i,m}^{me} - T_{i,m}^{ca})^2 - \left[\frac{1}{N \cdot M} \sum_{m=1}^M \sum_{i=1}^N (T_{i,m}^{me} - T_{i,m}^{ca}) \right]^2 \right\}^{1/2} \quad (16)$$

The preceding measurement errors do not occur in the steady-state tests. Models found from those tests are also applied to the transient tests and vice-versa and the aforementioned shifts are also partly due to unequal over-all heat input and output; therefore we have calculated μ by Eq. (16) for the cases presented in Table 7.

With three exceptions, the μ obtained by all new models is smaller than that for the initial model (0) even when these models are applied to the other tests. This is not necessarily to be expected, because only one thermocouple had been fixed on each node, and because the heat fluxes in the spacecraft are quite different during the different tests. No improvement is obtained when model V-4 is applied to

Table 5 Sums (rounded off) of residuals, of absolute residuals and of all terms

| Test Model | V-1 | | V-2 | | V-3 | | V-4 | | H-1 | | H-2 | | H-3 | |
|-------------------------|------|-----|------|-----|-------|-----|------|-----|------|-----|------|-----|-------|------|
| | 0 | V-1 | V-1 | V-2 | 0 | V-3 | 0 | V-4 | 0 | H-1 | H-1 | H-2 | 0 | H-3 |
| $\sum \Sigma r_{i,m}$ | -45 | 0 | 611 | 0 | -68 | 0 | -280 | 0 | -33 | 0 | 713 | 0 | 139 | 0 |
| $\sum \Sigma r_{i,m} $ | 254 | 54 | 1390 | 712 | 2237 | 912 | 1254 | 456 | 303 | 59 | 1081 | 508 | 3789 | 2290 |
| $\sum \Sigma s_{i,m}$ | 1922 | | 6831 | | 12254 | | 9189 | | 1934 | | 6584 | | 13345 | |

Table 6 Convergence of some factors and of the sum of the absolute residuals in test V-3

| Factor | Initially | After Eqs. (13-15) | After iteration | | | | |
|---------------------------|-----------|--------------------------|-----------------|------|------|------|------|
| | | | 1 | 2 | 3 | 4 | 5 |
| $E_1 \cdot 10^4$ | 1344 | 1369 | 1461 | 1460 | 1459 | 1458 | 1458 |
| $S_1 \cdot 10^2$ | 6949 | 7081 | 7242 | 7173 | 7138 | 7113 | 7093 |
| $A_1 \cdot 10^{12}$ | 2346 | 2326 | 2241 | 2260 | 2261 | 2258 | 2252 |
| $B_1 \cdot 10$ | 2970 | 3043 | 2348 | 2364 | 2346 | 2329 | 2316 |
| $C_{12} \cdot 10^4$ | 960 | | 1137 | 1166 | 1109 | 1080 | 1082 |
| $R_{12} \cdot 10^{13}$ | 54 | | 731 | 731 | 731 | 731 | 731 |
| $\Sigma \Sigma r_{i,m} $ | 2237 | 2244 | 1022 | 935 | 919 | 915 | 912 |

tests V-3, H-1, and H-2. This may perhaps be explained, in addition to the measuring error mentioned previously, by too large a time interval between the temperature measurements, which was 5 min in test V-4 (in all other transient tests, 2 min). As expected, the smallest deviations are situated on the diagonal; e.g., model V-2 gives the smallest deviation when applied to test V-2, from which it had been found. The aforementioned shifts are shown by the rms of the temperature differences, i.e., the first term of Eq. (16), $\Sigma_m \Sigma_i (T_{i,m}^{me} - T_{i,m}^{ca})^2 / (N \cdot M)$. The rms is obtained as 4.42, 4.27, 2.95, 4.66, 9.02, 7.54, when model V-3 is applied to tests V-1-V-4, H-1, and H-2, respectively.

Table 7 Standard deviation of differences between measured and calculated temperatures

| Test | V-1 | V-2 | V-3 | V-4 | H-1 | H-2 | H-3 |
|---------|------|------|------|------|-------|------|------|
| Model 0 | 9.34 | 7.99 | 5.22 | 6.46 | 9.81 | 7.66 | 5.08 |
| V-1 | 3.86 | 4.08 | | | 8.16 | 6.75 | |
| V-2 | 6.75 | 2.06 | | | 8.70 | | |
| V-3 | 4.41 | 4.08 | 2.94 | 4.19 | 8.76 | 7.48 | |
| V-4 | 7.72 | 7.34 | 6.11 | 5.41 | 11.58 | 9.86 | |
| H-1 | 8.97 | | | | 4.34 | | |
| H-2 | 8.11 | | | | 6.36 | 1.40 | |
| H-3 | 8.63 | | | | 5.80 | | 2.75 |

Because model V-3 is very good for all tests in the vertical position, and acceptable for tests in the horizontal position, it can probably best be used for the calculations in orbit, where the solar radiation very seldom falls parallel to the main axis of symmetry of the spacecraft and the temperatures of some components (e.g., solar cells) approach the design limits.

Conclusions

The study has shown that the method presented can be applied to an extended thermal mathematical model. It is simple, fast, and efficient (7 sec on the IBM/360 40H computer for one iteration over the 1957 parameters); however, it

does not permit the investigation of special phenomena such as representability of the thermal model (breakdown into nodes), experimental errors, etc. Some of the disagreements noted herein are certainly due to these phenomena. Moreover, engineering judgements are needed for choosing ranges, weighting factors, time intervals, etc. Nevertheless, some interesting results were found by analyzing seven different test conditions on the ESRO-I satellite.

In the stationary tests the sum of the residuals of the heat balance equations was reduced by a factor of 5, and in all transient tests, by a factor near 2 (Table 5). The standard deviation of the differences between the measured and calculated temperatures was reduced by a factor of 2 when a model was applied to the test from which it had been found (Table 7); however, if a model calculated from a test in which the solar radiation was normal to the spacecraft's spin axis was applied to a test in which this radiation was parallel to the spin axis, only a slight reduction was obtained.

The most generally valid model was found from a cyclic state in which the time interval between the temperature measurements was only 2 min. Then the rms of the differences between the measured and calculated temperatures and the standard deviation of these differences were reduced by a factor of about 2, which was also the case when the model was applied to other tests. Owing to the measuring errors, a heating (cooling) period gave higher (lower) heat capacities than the cyclic state (Table 3), as was explained. This shows that the thermal model of any spacecraft is best determined from a cyclic state. It is probably not necessary to wait till the cyclic state is exactly reached, since the analysis does not use the fact that the temperatures at the beginning of this state are equal to those at the end, but only the error-compensating effect. The analysis on a computer should be carried out concurrently with the thermal test, so that the test can be stopped when no further significant improvement in the predictions is possible.

References

- ¹ Toussaint, M. et al., "A Study of the Thermal Behaviour of the ESRO-I Satellite; Pt. I: The Mathematical Model," ESRO TN-20, 1967, European Space and Technology Centre, Noordwijk, Holland.
- ² Toussaint, M., Doenecke, J., and Martinet, J., "A Study of the Thermal Behaviour of the ESRO-I Satellite; Pt. II: Verification of the Mathematical Model," ESRO TN-21, 1968, European Space and Technology Centre, Noordwijk, Holland.
- ³ Toussaint, M., "Verification of the Thermal Mathematical Model for Artificial Satellites: A New Test Philosophy," *AIAA Progress in Astronautics and Aeronautics: Thermophysics of Spacecraft and Planetary Bodies*, Vol. 20, edited by G. B. Heller, Academic Press, New York, 1967, pp. 611-629.
- ⁴ Habermann, C. M., *Use of Digital Computers for Engineering Applications*, 1st ed., Merrill, Columbus, 1966, p. 190.